ACADEMIC PRESS

Available online at www.sciencedirect.com

SCIENCE DIRECT®

Journal of Sound and Vibration 264 (2003) 499–521

JOURNAL OF SOUND AND VIBRATION

www.elsevier.com/locate/jsvi

Prediction of acoustic fields radiated into a damped cavity by an *N*-port source through ducts ☆

M. Boudoy[a], V. Martin[b,*]

[a] *Faurecia Systèmes d'Echappement, Bois-sur-Près, 25550 Bavans, France*

[b] *Electromagnetism and Acoustics Laboratory, Swiss Federal Institute of Technology, Lausanne, CH-1015, Switzerland*

Received 28 January 2002; accepted 21 June 2002

Abstract

The use of two parameters—source impedance and source strength—to model a fluid machine radiating fluid-borne sound via ducts has led to excellent predictions when the source, a ventilator, propagates in one or two plane-wave ducts. Can such previously published methods successfully be applied to the case of a multi-port source radiating via ducts into a damped cavity? The case under study here is a car ventilation/heating unit and the aim was to predict the pressure spectrum inside the passenger compartment caused by the noise propagated through the ventilation ducts. The progressive validation procedure used indicated how and why as the system increases in complexity, predictive accuracy diminishes. The final results are nevertheless convincing and the hypotheses, which can be further refined to reflect the reality better and provide higher quality results, are clearly defined.

Introduction

In most propagation issues, the sources are considered to be the origin of the propagations, unaffected by them. In equations, the source terms are second members or boundary conditions. Thus, the moving part of a loudspeaker, strongly influenced by its acoustic load, cannot be considered as a source. To attempt to describe a fan in terms of source parameters is obviously more difficult than to describe a loudspeaker and characterizing such complex sources has long been a subject of study [1]. In the frequency domain, by analogy with electrical circuits, it is

☆ At its start, the project was carried out at Laboratoire de Mécanique de Rouen, CNRS-INSA de Rouen, Saint Etienne du Rouvray, F-76801, where both authors worked.

*Corresponding author. Vincent MARTIN, LEMA-DE, Swiss Federal Institute of Technology—Lausanne, CH-1015.

E-mail addresses: mboudoy@bavans.faurecia.com (M. Boudoy), vincent.martin@epfl.ch (V. Martin).

0022-460X/03/$ - see front matter
doi:10.1016/S0022-460X(02)01204-X

accepted intuitively that an acoustic source is a pressure generator with an internal impedance, and this will be demonstrated. In the electrical analogy the load is a scalar. In acoustics, under the plane-wave hypothesis, this scalar load is the radiation impedance transferred back from one extremity of a duct to the ventilator placed at the other. In this case, the source is called a *one-port source*. Implicitly, such a description rests on the linear and time-invariant behaviour of the source. For such a model to be used, it was necessary to find measurements which could identify the pressure and impedance parameters of the source itself. These two unknowns can be deduced by measuring the pressure resulting from just two distinct and known loads. Indeed, since there are two source data, there is now a system of two linear equations with two unknowns [2,3]. This method, which only uses the source to be identified, is rivalled by another which uses an external source. The latter method [4] is in two steps which consist, firstly, in measuring the source impedance by exciting the source with the sound field from an external source, and secondly, in determining the source strength without the external source by measuring the pressure when a known load (or several, to obtain a mean) is applied. The external source signal can be a harmonic noise in which case the measurements are taken frequency by frequency, or a random signal, where spectral densities have to be measured. The impedance measurements are taken according to the transfer function technique [5] which by-passes the need for acoustic velocity measurements. Note that in the case of a passive two-port, the measurements were taken with a transient signal [6].

When the ventilator propagates noise both downstream and upstream, it becomes a two-port source, which can be modelled as having one source upstream and one downstream as long as there is no interference between the two, in other words, among other things, as long as the load impedances are totally independent. In this case, the measurements to be taken are the same as those for a one-port source. Noise predictions in ducts obtained using this method can be of excellent quality, i.e., they agree perfectly with the measurements.

When, however, the source is truly a two-port source, the intuitive approach is no longer appropriate, and formulating the propagation operator will specify better what is meant by interaction or absence of interaction between the loads, and will provide the grounds for what will be needed to deduce the source parameters and ultimately obtain the propagation inside the passenger compartment .

Can this method be developed today for use with a source which has more than two ports, keeping the plane-wave hypothesis ? At each port, the load becomes a plane wave either because it is continued by a plane-wave duct, or because it is continued by a cone-shaped wide-mouthed duct. Such a situation exists in the automotive field with the vehicle air conditioning unit. Indeed, the air conditioning box usually has six exit ducts, directed towards the sides, the floor and the windscreen (the defrosting ducts) through which the sound propagates before it radiates inside the passenger compartment, which is considered a priori to be sufficiently damped for the loads to be independent.

It should be emphasized here that source characterization is only the first step in the development of a global predictive methodology. Previous work has been done on the prediction of the pressure spectrum radiated in a free space through a duct connected to a one-port source [7], and on calculation of the sound generated in ducts by a two-port source [8,9]. The question is to find out how to extend these previous works to the case of a multi-port sound source connected with ducts radiating inside a damped cavity.

It is this global predictive problem, split into two parts, which is presented in this paper. The methodology is first generalized to a multi-port source connected to one-dimensional (1-D) pipes, and then to the case of two wide-mouthed ducts, where the plane wave is no longer the only propagative mode. The measurements taken in each case are the same as those taken for a two-port source.

In Section 2, a simple presentation is given, defining the source pressure and impedance in the case of a one-port source, while in no way detracting from the generality of the approach. The principle of the measurements necessary to determine source pressure and impedance arises from the formulation. We then proceed to carry out the actual measurements, justifying the different techniques chosen. Subsequently, by formulating the propagation operators inside the cavity, the method for measuring the radiation impedance of the duct inside the cavity is derived, and the transfer path between the duct exit and the target points in the cavity is determined.

In Section 3, the formulation will be generalized to two-port sources, with attention being paid to the question of load coupling which could be significant here. The measurements in this case also derive from the formulation. All the elements will now be in place to tackle experimentally the problem of a four-port source, each being loaded by impedances transferred back through a plane-wave duct.

Finally, in Section 4, we will deal with the case of the noise from the defrosting ducts with the propagation modelled as a two-port source with impedances transferred back via multi-modal guides. Predictive pressure spectra will be compared with in situ measurements.

Although the prediction results are satisfactory, as the system increases in complexity, the accuracy of the prediction diminishes and the progressive procedure adopted shows the areas where further improvements in the method can be made. Nevertheless, there is no doubt that the strategy presented to tackle the global problem is entirely appropriate and our conclusion gives the reasons for our confidence in it. As far as we know, the methodology used to deal with the case studied has not so far been generalized nor has attention yet been drawn to its main features.

Before starting on the subject, some clarification regarding the use of the word "prediction", frequent in this paper, is needed. The procedure presented consists in treating the whole acoustic domain by assembling sub-domains. By analogy, in linear algebra a global matrix may be dealt with by sub-structuration, whereby the solution must be the same as that obtained from the whole matrix. To ascertain that this is the case amounts to numerical verification. Similarly in this study, if all acoustic characteristics of each sub-domain result from measurements, the assembling ought to lead to the results measured in the whole domain (as long as the measurements are perfect and linearity is present). To ascertain that this is the case would amount to experimental verification. On the contrary, when one (or more) sub-domain(s) is modelled either by equations describing physical phenomena and/or by approximate numerical methods, the assembly of all sub-domains will not necessarily lead to the measured result in the whole domain. In this case, the results arising from the assembly constitutes a prediction that will be compared with the measured reality which amounts to experimental validation. However, when modelling the sub-domain gives a well-known reliable description, the term "prediction" is perhaps not totally appropriate.

2. One-port source radiating in a cavity via a plane waveguide

Let us consider the case of two cavities Ω_1 and Ω_3 coupled by duct Ω_2 in the context of a vehicle ventilation system (Fig. 1). A sound source is connected to the first cavity Ω_1 at section S. The connection sections between Ω_1 and Ω_2, and between Ω_2 and Ω_3 are respectively, Γ_A and Γ_B.

The global problem, in its most simplified form associated with some drastic hypothesis could be written as follows: considering $\Omega \equiv \Omega_1 \cup \Omega_2 \cup \Omega_3$ of internal surface $\partial\Omega$ with a sound source at section S, the acoustic operator for acoustic pressure $p(\mathbf{x})$ inside Ω could be

$$\begin{aligned} &Hp(\mathbf{x}) = (\Delta + k^2)p(\mathbf{x}) = 0 \quad \text{in } \Omega, \\ &p_{,n} = -\mathrm{i}\rho\omega v_n \quad \text{on } S, \\ &p_{,n} = 0 \quad \text{on } \partial\Omega \setminus S, \end{aligned}$$

where $\mathrm{i} = \sqrt{-1}$, ω is the radian frequency, k the wave number, ρ the density of the medium, $p_{,n}$ is the spatial partial derivative of the pressure along the normal, and v_n the acoustic normal velocity. The ratio $p/(\rho c v_n)$ is called the specific acoustic impedance and the inverse is the specific admittance noted β.

More precisely, inside volume Ω_1, with an acoustic load of impedance Z_A on Γ_A and with source S active, a more general acoustic operator for acoustic pressure $q(\mathbf{x})$ could be

$$\begin{aligned} &Hq(\mathbf{x}) = 0 \quad \text{in } \Omega_1, \\ &q_{,n} + \mathrm{i}k\beta_\sigma q = f \quad \text{on } S, \\ &q_{,n} + \mathrm{i}k\beta_A q = 0 \quad \text{on } \Gamma_A, \\ &q_{,n} + \mathrm{i}k\beta_1 q = 0 \quad \text{on } \partial\Omega_1 \setminus (S \cup \Gamma_A), \end{aligned} \tag{1}$$

which is solved by using the Green function $g(\mathbf{x},\mathbf{x}')$ of cavity Ω_1 which, for example, satisfies the same passive boundary conditions as $q(\mathbf{x})$ on $\partial\Omega_1 \setminus \Gamma_A$:

$$\begin{aligned} &H_x g(\mathbf{x},\mathbf{x}') = \delta(\mathbf{x},\mathbf{x}') \quad \text{in } \Omega_1, \\ &g_{,n} + \mathrm{i}k\beta_\sigma g = 0 \quad \text{on } S, \\ &g_{,n} + \mathrm{i}k\beta_1 g = 0 \quad \text{on } \partial\Omega_1 \setminus S \end{aligned}$$

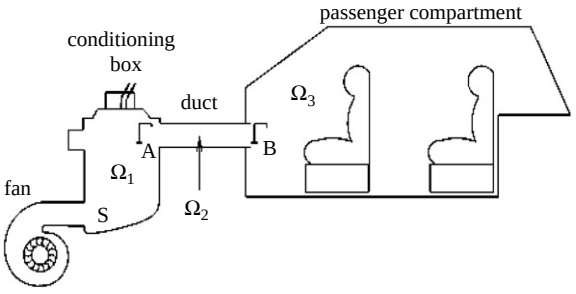

Fig. 1. Schematic diagram of the car ventilation system with only one duct.

resulting in the boundary equation for acoustic pressure $q(\mathbf{x})$ inside Ω_1:

$$q(\mathbf{x}) = -\int_S g(\mathbf{x},\mathbf{x}')f(\mathbf{x}')\,\mathrm{d}\mathbf{x}' - \mathrm{i}k(\beta_1-\beta_A)\int_{\Gamma_A} q(\mathbf{x}')g(\mathbf{x},\mathbf{x}')\,\mathrm{d}\mathbf{x}'.$$

Assuming a uniform acoustic field on section Γ_A, this equation for pressure q_A on Γ_A becomes

$$q_A = -\frac{\int_S g(\mathbf{x}_A,\mathbf{x}')f(\mathbf{x}')\,\mathrm{d}\mathbf{x}'}{1+\mathrm{i}k\beta_1\int_{\Gamma_A} g(\mathbf{x}_A,\mathbf{x}')\,\mathrm{d}\mathbf{x}'} + \mathrm{i}k\frac{\int_{\Gamma_A} g(\mathbf{x}_A,\mathbf{x}')\,\mathrm{d}\mathbf{x}'}{1+\mathrm{i}k\beta_1\int_{\Gamma_A} g(\mathbf{x}_A,\mathbf{x}')\,\mathrm{d}\mathbf{x}'}\beta_A q_A, \tag{2}$$

$$q_A = p_s + Z_s\,\beta_A q_A, \tag{3}$$

$$q_A = \frac{p_s}{(1-Z_s\beta_A)}, \tag{4}$$

where p_s is the source pressure and Z_s the source impedance. Both parameters are independent of the load applied on Γ_A. It should be noted that with another elementary solution $g'(\mathbf{x},\mathbf{x}')$ which satisfies, for instance, the operator

$$\begin{aligned} &H_x g'(\mathbf{x},\mathbf{x}') = \delta(\mathbf{x}-\mathbf{x}') \quad \text{in } \Omega_1,\\ &g'_{,n} + \mathrm{i}k\beta_1 g' = 0 \qquad\quad \text{on } \partial\Omega_1, \end{aligned}$$

the expressions for p_s and Z_s would be more complicated but would obviously not change the value of these parameters.

From Eq. (3), a test procedure for measuring source parameters p_s and Z_s can be directly deduced. Indeed, this equation is linear relative to the unknowns p_s and Z_s, so the measurement of pressure q_A and of load admittance β_A with successively two different load conditions leads to the source parameters. Using more than two loads induces over-determination which increases the accuracy of the results [10,11], but Shridha and Crocker [12] have highlighted the weaknesses of this method. Another solution is to use a two-step procedure, the first step consisting in measuring the source impedance Z_s with the help of an external sound source connected to section Γ_A. In the second step, the source pressure is deduced from a measurement of q_A and from the previous determination of Z_s by applying a known acoustic load on Γ_A. Using more than one load allows the results to be averaged.

The boundary equations can be used to clarify the source impedance determination method with an external source. When the main source S is turned off and the external source is turned on, the acoustic pressure $r(\mathbf{x})$ inside Ω_1 verifies the following system:

$$\begin{aligned} &Hr(\mathbf{x}) = 0 \qquad\quad \text{in } \Omega_1,\\ &r_{,n} + \mathrm{i}k\beta_\sigma r = 0 \quad \text{on } S,\\ &r_{,n} + \mathrm{i}k\beta_\gamma r = h \quad \text{on } \Gamma_A,\\ &r_{,n} + \mathrm{i}k\beta_1 r = 0 \quad \text{on } \partial\Omega_1 \setminus (S\cup\Gamma_A). \end{aligned} \tag{5}$$

Writing the boundary equation for pressure r_A on section Γ_A, with the assumption that the acoustic pressure and velocity fields on section Γ_A are uniform, yields

$$r_A = -\mathrm{i}k\beta_1 r_A\int_{\Gamma_A} g(\mathbf{x}_A,\mathbf{x}')\mathrm{d}\mathbf{x}' - r_{,nA}\int_{\Gamma_A} g(\mathbf{x}_A,\mathbf{x}')\,\mathrm{d}\mathbf{x}'$$

or

$$-ik\frac{r_A}{r_{,nA}} = \frac{\mathrm{i}k\int_{\Gamma_A} g(\mathbf{x}_A,\mathbf{x}')\,\mathrm{d}\mathbf{x}'}{1+\mathrm{i}k\beta_1\int_{\Gamma_A} g(\mathbf{x}_A,\mathbf{x}')\;\mathrm{d}\mathbf{x}'} = Z_s. \tag{6}$$

It is worth noting that both the admittance β_γ and the solicitation h are included in the term $r_{,nA}$. The above equation, in association with Eq. (2), shows that the source impedance can be obtained by connecting an external sound source to section Γ_A and by measuring the resulting impedance on this section. In practice, the source impedance is deduced from the measurement of a transfer function between two pressure signals at two microphones located in a duct connecting the external sound source to section Γ_A, using to the transfer function technique [5]. With an antenna of three microphones instead of two, flow noise is suppressed by measuring the coherence functions between each sensor.

When the pressure on Γ_A is sought via Eq. (4), with the source parameters p_s and Z_s being previously measured, the last parameter to be determined is the load admittance β_A. It is calculated by transferring the impedance Z_B on section Γ_B back to section Γ_A with the help of the duct transfer matrix. The main difficulty is to obtain the admittance on section Γ_B as the latter reveals the acoustic behaviour of the cavity Ω_3 which may be quite complex. Again, a better clarity of the situation is obtained by writing the acoustic operator over pressure $s(\mathbf{x})$ in cavity Ω_3 as isolated from the rest of the system and with an external sound source connected to section Γ_B:

$$\begin{aligned} &Hs(\mathbf{x}) = 0 && \text{in } \Omega_3,\\ &s_{,n} + \mathrm{i}k\beta_\mu \mathrm{s} = \mathrm{e} && \text{on } \Gamma_B,\\ &s_{,n} + \mathrm{i}k\beta_3 \mathrm{s} = 0 && \text{on } \partial\Omega_3 \setminus \Gamma_B. \end{aligned} \tag{7}$$

Let us call g_3 the Green function of cavity Ω_3 which verifies the following system:

$$\begin{aligned} &H_x g_3(\mathbf{x},\mathbf{x}') = \delta(\mathbf{x}-\mathbf{x}') && \text{in } \Omega_3,\\ &g_{3,n} + \mathrm{i}k\beta_3 g_3 = 0 && \text{on } \partial\Omega_3. \end{aligned}$$

The boundary equation with the uniform acoustic field over Γ_B, leads to:

$$-\mathrm{i}k\frac{s_\mathrm{B}}{s_{,nB}} = Z_B = \frac{\mathrm{i}k\int_{\Gamma_B} g_3(\mathbf{x}_B,\mathbf{x}')\,\mathrm{d}\mathbf{x}'}{1+\mathrm{i}k\beta_3\int_{\Gamma_B} g_3(\mathbf{x}_B,\mathbf{x}')\,\mathrm{d}\mathbf{x}'} \tag{8}$$

If the cavity geometry and behaviour are simple enough for Green function g_3 and wall admittance β_3 to be perfectly known, impedance Z_B is calculated. Otherwise it is measured in the same way as the source impedance was, i.e., by using the transfer function technique.

Knowing the three parameters p_s, Z_s and β_A, the sound pressure on section Γ_A results from Eq. (4). However, in most cases, the pressure spectrum inside cavity Ω_3 is sought, which is why pressure q_A is propagated towards section Γ_B via the duct transfer matrix in order to obtain q_B. Then acoustic pressure q_3 on the target point $\mathbf{x}_3$ in cavity Ω_3 can be calculated if the transfer

function $Q(\mathbf{x}_3)$ between section Γ_B and $\mathbf{x}_3$ is available as $q_3 = Q(x_3)q_B$. This transfer function $Q(\mathbf{x}_3)$ is determined with cavity Ω_3 isolated from the rest of the system. Writing the boundary equation associated with acoustic operator (7) for target point $\mathbf{x}_3$ inside Ω_3, one obtains after several simplifications:

$$Q(\mathbf{x}_3) = \frac{s(\mathbf{x}_3)}{s_B} = -\mathrm{i}k\frac{\beta_3 Z_B - 1}{Z_B}\int_{\Gamma_B} g_3(\mathbf{x}_3, \mathbf{x}')\,\mathrm{d}\mathbf{x}' \tag{9}$$

Once again, if cavity Ω_3 is simple enough for the Green function g_3 to be perfectly known, the transfer function $Q(\mathbf{x}_3)$ is calculated. Otherwise, it is measured.

To sum up, the prediction of the acoustic pressure inside Ω_3 follows this procedure:

- The source parameters p_s and Z_s are determined as well as the cavity parameters Z_B and $Q(\mathbf{x}_3)$ which can be calculated or measured. The duct transfer matrix is also calculated.
- The load impedance on Γ_B is transferred back to section Γ_A thanks to the duct transfer matrix. Then, Eq. (4) results in the acoustic pressure on Γ_A, which is propagated through Ω_2 towards section Γ_B in order to obtain pressure q_B. Finally, the acoustic pressure on the target point of cavity Ω_3 is the product of q_B and $Q(\mathbf{x}_3)$.

To conclude this section, it should be pointed out that the acoustic operators were chosen for the sake of simplicity, but this does not affect the generality of the procedure.

3. Multi-port sound source connected to a cavity via several plane waveguides

3.1. The specificities of an N-port source

Having dealt with the presentation of a one-port source in the previous section, we now focus on a cavity Ω_1 with N exits, called a N-port source. The whole system configuration, in the case of a two-port source, is shown in Fig. 2 (again in the frame of the automotive industry). The two exit sections of Ω_1 are called Γ_A and Γ_C while the two entry sections of the main cavity

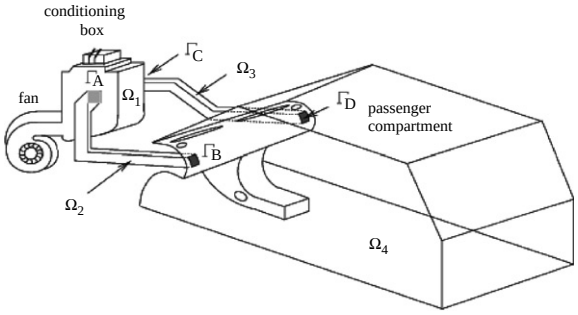

Fig. 2. Schematic diagram of the car ventilation system with two lateral ducts.

Ω_4 are Γ_B and Γ_D. The acoustic operator for pressure $q(\mathbf{x})$ inside Ω_1 is, for instance:

$$\begin{aligned} &Hq(\mathbf{x}) = 0 && \text{in } \Omega_1,\\ &q_{,n} + \mathrm{i}k\beta_\sigma q = f && \text{on } S,\\ &q_{,n} + \mathrm{i}k\beta_A q = 0 && \text{on } \Gamma_A,\\ &q_{,n} + \mathrm{i}k\beta_C q = 0 && \text{on } \Gamma_C,\\ &q_{,n} + \mathrm{i}k\beta_1 q = 0 && \text{on } \partial\Omega_1 \setminus (S \cup \Gamma_A \cup \Gamma_C). \end{aligned} \tag{10}$$

Here also, this particular operator does not affect the generality of the demonstration as long as the load impedances on sections Γ_A and Γ_C are independent. The case of dependent loads will be tackled later on. Let us call $g(\mathbf{x},\mathbf{x}')$ the Green function of cavity Ω_1 which verifies the operator:

$$\begin{aligned} &H_x g(\mathbf{x},\mathbf{x}') = \delta(\mathbf{x}-\mathbf{x}') && \text{in } \Omega_1,\\ &g_{,n} + \mathrm{i}k\beta_\sigma g = f && \text{on } S,\\ &g_{,n} + \mathrm{i}k\beta_1 g = 0 && \text{on } \partial\Omega_1 \setminus S. \end{aligned}$$

The acoustic field is regarded as uniform on Γ_A and Γ_C so the acoustic pressures on Γ_A and Γ_C are called p_A and p_C, respectively. Inserting the notation simplifications $g_A = g(x_A;\cdot)$, $g_C = g(x_C,\cdot)$, classical calculation yields

$$\begin{Bmatrix} p_A \\ p_C \end{Bmatrix} = -\underbrace{\begin{Bmatrix} \int_S g_A f \\ \int_S g_C f \end{Bmatrix}}_{\{\mathbf{f}_s\}} - \mathrm{i}k \underbrace{\begin{bmatrix} \int_{\Gamma_A} g_A & \int_{\Gamma_C} g_A \\ \int_{\Gamma_A} g_C & \int_{\Gamma_C} g_C \end{bmatrix}}_{[\mathbf{M}]} \left(\beta_1 - \underbrace{\begin{bmatrix} \beta_A & 0 \\ 0 & \beta_C \end{bmatrix}}_{[\boldsymbol{\beta}]} \right) \begin{Bmatrix} p_A \\ p_C \end{Bmatrix},$$

i.e.,

$$\begin{Bmatrix} p_A \\ p_C \end{Bmatrix} = \underbrace{\left([\mathbf{I}] + \mathrm{i}k\beta_1[\mathbf{M}]\right)^{-1}\{\mathbf{f}_S\}}_{\{\mathbf{p}_s\}} + \underbrace{\mathrm{i}k\left([\mathbf{I}] + \mathrm{i}k\beta_1[\mathbf{M}]\right)^{-1}[\mathbf{M}]}_{[\mathbf{Z}_s]} \underbrace{[\boldsymbol{\beta}]\begin{Bmatrix} p_A \\ p_C \end{Bmatrix}}_{-1/\mathrm{i}k\begin{Bmatrix} p_{,nA} \\ p_{,nC} \end{Bmatrix}} \tag{11}$$

or, in matrix notation:

$$\mathbf{p} = \mathbf{p}_s + \mathbf{Z}_s\mathbf{Z}_l^{-1}\mathbf{p}. \tag{12}$$

In the case of signals that are random functions of time, Eq. (12) is modified by considering spectrum and cross-density matrices ($\mathbf{S}_s$ and $\mathbf{S}$) as variables instead of acoustic pressure vectors ($\mathbf{p}_s$ and $\mathbf{p}$):

$$\mathbf{S}_s = \mathbf{p}_s(\mathbf{p}_s)^c = \begin{pmatrix} S^s_{AA} & S^s_{AC} \\ S^s_{CA} & S^s_{CC} \end{pmatrix} \quad \text{and} \quad \mathbf{S} = \mathbf{p}(\mathbf{p})^c = \begin{pmatrix} S_{AA} & S_{AC} \\ S_{CA} & S_{CC} \end{pmatrix},$$

where superscript c refers to the conjugate transpose. Eq. (12) is thus transformed into

$$\mathbf{S}_s = (\mathbf{1} + \mathbf{Z}_s\mathbf{Z}_l^{-1})^{-1}\mathbf{S}\left[(\mathbf{1} + \mathbf{Z}_s\mathbf{Z}_l^{-1})^c\right]^{-1}. \tag{13}$$

The load matrix $[\beta]$ (and $\mathbf{Z_l} = [\beta]^{-1}$) is diagonal due to the assumption of independent loads on Γ_A and Γ_C, but it is worth mentioning that the boundary conditions may have the

following form:

$$\begin{Bmatrix} p_{,nA} \\ p_{,nC} \end{Bmatrix} + \mathrm{i}k \begin{bmatrix} \beta_{AA} & \beta_{AC} \\ \beta_{CA} & \beta_{CC} \end{bmatrix} \begin{Bmatrix} p_A \\ p_C \end{Bmatrix} = \begin{Bmatrix} 0 \\ 0 \end{Bmatrix} \text{ on } \Gamma_A \text{ and } \Gamma_C.$$

This form occurs, in particular when the two guides end in the same cavity (here Ω_4). Nevertheless, it has been assumed that the guide exits Γ_B and Γ_D are spaced out enough for the extra-diagonal terms of matrix $[\beta]$ to be negligible compared to the diagonal terms.

Concerning the relation between $\mathbf{Z}_s$ and $\mathbf{M}$, it should be noted that $\mathrm{i}k\mathbf{M}$ is the source impedance matrix, where the inner walls of Ω_1 are rigid.

The procedure used to measure source parameters $\mathbf{S}_s$ and $\mathbf{Z}_s$ originates from that used in the one-port source case. Indeed, it is a two-step test procedure, with an external sound source to measure the source impedance matrix. Here matrix $\mathbf{Z}_s$ has four components and two different acoustic configurations are needed. They are obtained by putting the external source successively at each exit of Ω_1 (i.e., Γ_A and Γ_C). Again, the antennae of three microphones placed on Γ_A and Γ_C, and the measurement of two transfer functions with the associated coherence functions for each loudspeaker position determine the source impedance matrix. Concerning the measurement of source strength matrix $\mathbf{S}_s$, two loads of known impedances are connected to Γ_A and Γ_C, and $\mathbf{S}_s$ is obtained without an external loudspeaker by measuring the auto and cross-spectrum densities as well as the associated coherence functions at the exits of Ω_1. Several pairs of loads allow the results to be averaged.

What is the difference between two one-port sources and a two-port source? If matrix $\mathbf{M}$, and consequently matrix $\mathbf{Z}_s$, is diagonal, Eq. (12) is equivalent to two one-port source equations (3) for Γ_A and Γ_C. This means that the load on Γ_C would have no impact on the acoustic pressure and velocity on Γ_A and conversely. Therefore, the extra-diagonal terms of matrix $\mathbf{Z}_s$ relative to the diagonal terms quantify the coupling of the guide entrances Γ_A and Γ_C through the cavity Ω_1. For instance, a fan in a duct would act as two one-port sources if the radiations upstream and downstream were independent, but this absence of coupling can only be judged after the source matrix of the two-port source has been measured.

3.2. Radiation of the multi-port source in a cavity via plane waveguides

To calculate the auto and cross-spectrum densities matrix $\mathbf{S}$ at the cavity Ω_1 exits, the load impedance matrix $\mathbf{Z}_l$ has to be determined. It is obtained by transferring impedance matrix $\mathbf{Z}_4$ at the duct exits back to the duct entrances via the duct transfer matrices. The impedance matrix $\mathbf{Z}_4$ reveals the acoustic behaviour of cavity Ω_4. The description of this behaviour in terms of acoustic operator and boundary equations will illustrate this effect. Let us consider that cavity Ω_4 is isolated from the rest of the system and that an external sound source is connected to section Γ_B. An acoustic operator of this configuration is

$$\begin{aligned} &Hq(\mathbf{x}) = 0 && \text{in } \Omega_4, \\ &q_{,n} + \mathrm{i}k\beta_\nu q = \mathrm{e} && \text{on } \Gamma_B, \\ &q_{,n} + \mathrm{i}k\beta_\mu q = 0 && \text{on } \Gamma_D, \\ &q_{,n} + \mathrm{i}k\beta_4 q = 0 && \text{on } \partial\Omega_4 \setminus (\Gamma_B \cup \Gamma_D). \end{aligned} \tag{14}$$

As previously, writing the boundary equation associated with this configuration, with the hypothesis that the acoustic fields on sections Γ_B and Γ_D are uniform, the following system of equations is obtained:

$$-\mathrm{i}k\begin{Bmatrix} q_B \\ q_D \end{Bmatrix} = \mathrm{i}k\big([I] + \mathrm{i}k\beta_4[M_4]\big)^{-1}[M_4]\begin{Bmatrix} q_{,nB} \\ q_{,nD} \end{Bmatrix} \text{ with } [Z_4] = \mathrm{i}k\big([I] + \mathrm{i}k\beta_4[M_4]\big)^{-1}[M_4], \quad (15)$$

where the components of matrix $\mathbf{M}_4$ are integrals of the Green function $g_4(\mathbf{x},\mathbf{x}')$ of Ω_4 (g_4 is built similarly to g_3 in Section 2).

When cavity Ω_4 has a geometry such that the Green function g_4 and the wall admittance β_4 are calculated, then matrix $\mathbf{Z}_4$ is also calculated. Otherwise, it is measured with a test procedure similar to that used to measure the source impedance matrix.

The second step in characterizing the cavity determines the transfers $Q_B(\mathbf{x}_4)$ and $Q_D(\mathbf{x}_4)$ between the duct exit sections Γ_B and Γ_D, and the target point $\mathbf{x}_4$ in Ω_4. If again the boundary equations associated with the acoustic operator (14) are considered, pressure at point x_4 is

$$q(\mathbf{x}_4) = -\mathrm{i}k\left(\beta_4\left\langle\int_{\Gamma_B} g_4, \int_{\Gamma_D} g_4\right\rangle[Z_4] - \left\langle\int_{\Gamma_B} g_4, \int_{\Gamma_D} g_4\right\rangle\right)[Z_4]^{-1}\begin{Bmatrix} q_B \\ q_D \end{Bmatrix}$$

or

$$q(x_4) = \langle Q_B(\mathbf{x}_4), Q_D(\mathbf{x}_4)\rangle\begin{Bmatrix} q_B \\ q_D \end{Bmatrix}.$$

According to the geometry of the cavity, $Q_B(\mathbf{x}_4)$ and $Q_D(\mathbf{x}_4)$ will either be calculated or measured. In the second case, the external loudspeaker will be successively put on Γ_B and on Γ_D.

Below, the procedure for predicting the pressure spectrum at a target point of Ω_4 caused by the radiation of a multi-port source via plane-wave ducts is summed up:

- Measurement of source parameters: Source impedance matrix $\mathbf{Z}_s$ and source strength matrix $\mathbf{S}_s$ of the N-port-source consisting of cavity Ω_1 with N exits are measured.
- Determination of cavity Ω_4 parameters
  –Radiation impedance matrix $\mathbf{Z}_4$ at cavity Ω_4 openings is calculated or measured.
  –Transfer functions between each cavity opening and the target points are measured.
- Prediction of the acoustic spectrum at the cavity target points
  –Load impedance matrix $\mathbf{Z}_1$ is calculated by transferring matrix $\mathbf{Z}_4$ back to the duct entrances with the help of the duct transfer matrices.
  –As all the needed parameters are known, Eq. (13) gives the auto and cross-spectrum density matrix at cavity Ω_1 exits.
  –The latter propagates to the cavity Ω_4 openings thanks to the duct transfer matrix resulting in $\mathbf{S}_4$.
  –Pressure spectrum at the cavity target points is calculated as

$$S(\mathbf{x}_4) = \sum_{i=B,D}\sum_{j=B,D} Q_i(\mathbf{x}_4)\ Q_j(\mathbf{x}_4)^* S_4^{i,j}.$$

3.3. Experimental results

As already mentioned, the motivation behind this work was in the prediction of the sound pressure spectrum inside the passenger compartment caused by the radiation of the air-conditioning box. The experimental results are to show to what extent the theoretical approach described in the last section fits the complex reality of a technological object such as an automobile air-conditioning system. At this stage, the defrosting ducts are not taken into account as they have too large an exit nor are the central ventilators which are too short for the single plane wave to be established. The air-conditioning box considered in this chapter is thus a four-port source with its four exits towards the lateral and floor level air ducts.

3.3.1. Experimental results in a semi-technological situation

The method to measure the multi-port source parameters was first validated in a semi-technological situation consisting of the air-conditioning system removed from the car and freely radiating in an anechoic chamber via straight guides. For this experiment, three ports of the air-conditioning box are considered: the left lateral, the right defrosting and the left floor-level exits. The other exits are not closed but connected to absorbent stoppers. The fan rotation was set at about half the maximum speed which induces an air flow speed at the car air outlets of between 3.2 and 4.2 m/s.

The source impedance matrix and the source strength matrix were measured successively with three different sets of loads (ducts of various lengths and expansion chambers) in order to average the results. The modulus of the source impedance matrix terms and the diagonal terms of the source strength matrix are shown in Figs. 3 and 4 respectively. It is seen that the three curves for the various sets of loads can be superimposed indicating that the source parameters are independent of the loads and that the measurements are correct.

A comparison in Fig. 5 of the predicted and measured sound pressure spectra just at the extremity of straight ducts or of an expansion chamber connected to the conditioning box and freely radiating into the anechoic room shows a very good correlation. It indicates that the hypothesis of the source linear behaviour is fulfilled.

Fig. 6 gives a comparison between the predicted and the directly measured spectra now with real ventilation ducts minus the defrosting duct. The results are of slightly poorer quality than those in Fig. 5, but they are still convincing. The loss of quality arises mainly from the difficulty in calculating the transfer function of the car ventilation ducts accurately due to their complex geometry (their section varies continually; the bends are not concentric).

It should be mentioned that, in the present experiment, the predicted results with three one-port sources are similar to those obtained with a three-port source. As seen in the previous section, this is because the off-diagonal terms of the source impedance matrix are, for most of the frequencies, negligible in comparison with the diagonal terms as can be seen on Fig. 3, and also because the duct exits are considered to be independent as they freely radiate in an anechoic room, so the load impedance matrix is diagonal. Nevertheless, the diagonality of the source impedance matrix for the three-port source may be specifically linked to this configuration and it should not be assumed that this would still be the case with other box exits. Moreover, further experimental results on a six-port source have shown that $\mathbf{Z}_s$ is not diagonal if the ports are located close to each other.

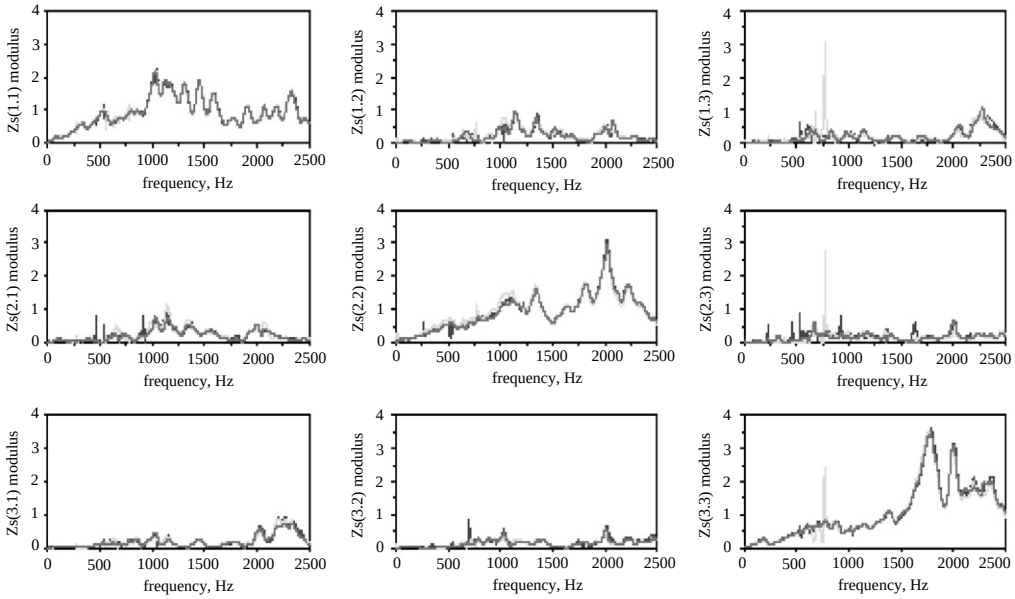

Fig. 3. Modulus of the source impedance matrix $\mathbf{Z}_s$.

3.3.2. *Experimental results in a technological situation*

Another experimental validation of the methodology was carried out on a complete vehicle, from which the central and the defrosting ducts had been removed. With these conditions, the noise predicted inside the passenger compartment was caused by the ventilation sound guided through the two lateral and two floor-level ducts. Fig. 7 shows a diagram of the air-conditioning box and of the ventilation ducts.

The source parameters derive from measurements taken on the global six-port source, made up of the conditioning box at the two lateral, two floor-level and two defrosting exits. These measurements were taken in a normal (i.e., non-anechoic room) so the source parameters are less well defined than those of the three-port source in Figs. 3 and 4.

The measurements on the vehicle (passenger compartment characterization and direct sound level measurements) were made in a semi-anechoic chamber. The transfers between the air outlets and the target points were obtained by connecting a loudspeaker emitting a white noise to the rear of the considered air outlet and by measuring the transfer functions between the pressure signals of a microphone in front of the outlet and others at the target points of the passenger compartment. The experimental set-up for this transfer measurement is shown in Fig. 8 (the microphones at the target points are not drawn). Two target points were located at the driver's left ear level and at the front passenger's right ear level (80 cm above the lower part of the seat and a 10 cm lateral shift from the middle of the headrest). The third target point was halfway between the two others.

Regarding how the radiation impedance matrix at the ventilation duct exit sections was determined, as the passenger compartment is of complex shape and partly absorbent, it was decided to approximate this matrix by a diagonal matrix composed of the impedance of a guide

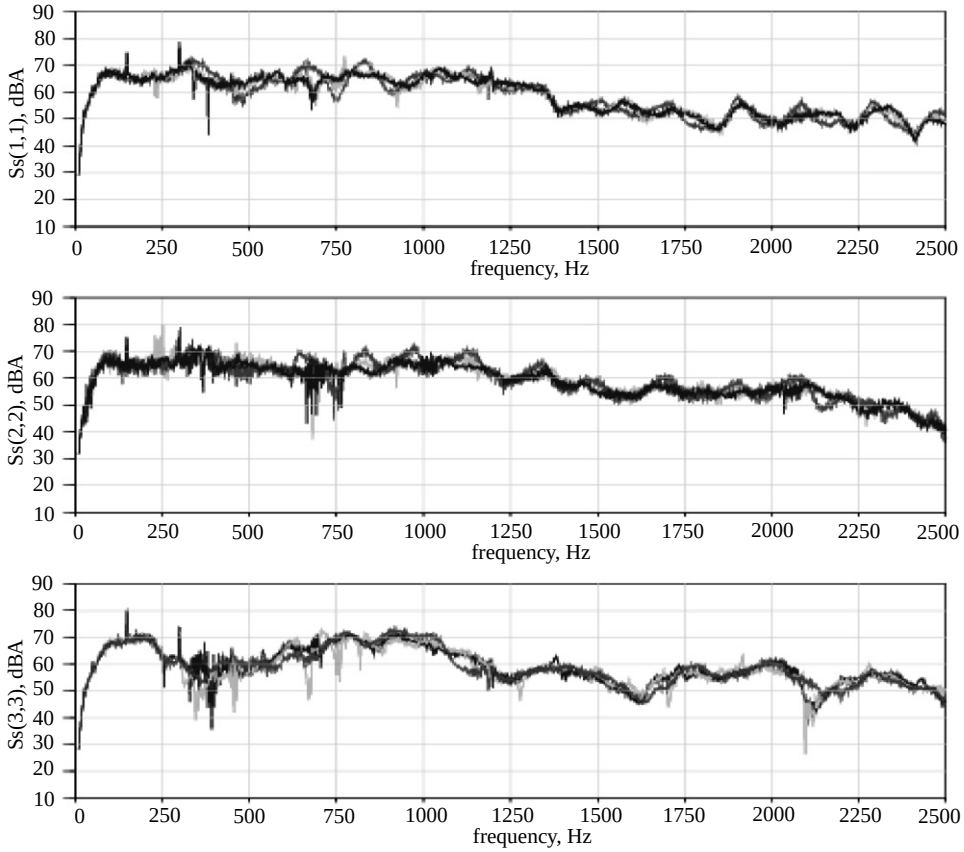

Fig. 4. Modulus of the diagonal terms of the source strength matrix.

running into a half-space limited by an infinite plane intended to model the influence of the dashboard.

The predicted sound pressure spectra from lateral and floor-level air outlets are compared to direct measurements of the auto-spectra on the three microphones at the target points of the passenger compartment. The curves are superimposed in Fig. 9. It appears that the correlation between predictive calculation and direct measurements is good, except in frequencies lower than 200 Hz. Beyond the dependent charges, this lack of correlation for low frequencies could be explained by the fact that, for direct measurements, the microphones were not protected with round windscreens when they were under the lateral outlets air flow. Indeed, two remarks results from experiments. On the one hand the difference between predictions and measured results for low frequencies is greater at the passenger headrest where the air flow speed is 3.6 m/s than at the driver headrest where the air flow speed is 3 m/s. Concerning the third microphone at the middle that receive less air flow, the difference is the smaller. On the other hand, the direct measurement for microphones at the headrests were more noisy than for the third microphone at the middle. The two phenomena could be related and if so, the use of windscreens would have led to better

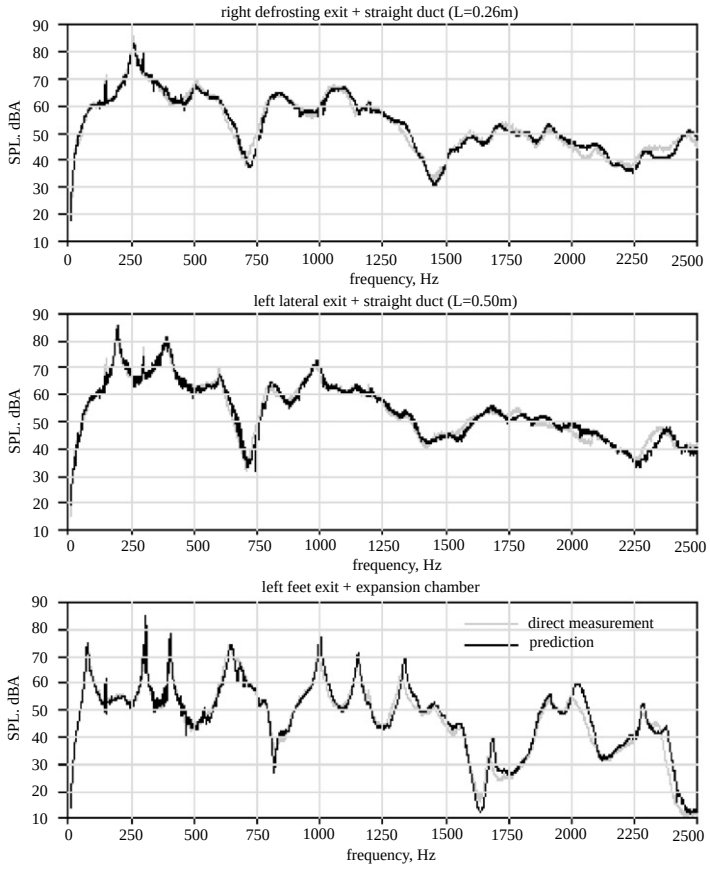

Fig. 5. Predicted and directly measured pressure spectra at the end of simple ducts connected to the three-port source.

measurements and perhaps would have diminished the differences with the predictions. For frequencies greater than 200 Hz, the measurements are of poorer quality than the results predicted at the end of ducts outside the vehicle (see Fig. 6). Two reasons can be reasonably suspected. The source parameters were not measured in an anechoic room nor with a sufficiently powerful external loudspeaker and they are thus tainted with slightly more experimental noise than those in Figs. 3 and 4. Moreover, modelling the ventilation ducts, and the passenger compartment with a half-space for the medium and high frequencies, might not be quite satisfactory. The latter reason is probably of the second order compared to the former. There, is however, no doubt that the accuracy of the results, sufficient here for our needs, can be improved if needed.

4. Two-port source connected to a cavity via two multi-modal guides

As seen in Sections 2 and 3, the acoustical model of multi-port sources implies a uniform acoustic field on each port. When the ducts connected to the ports are plane waveguides, this

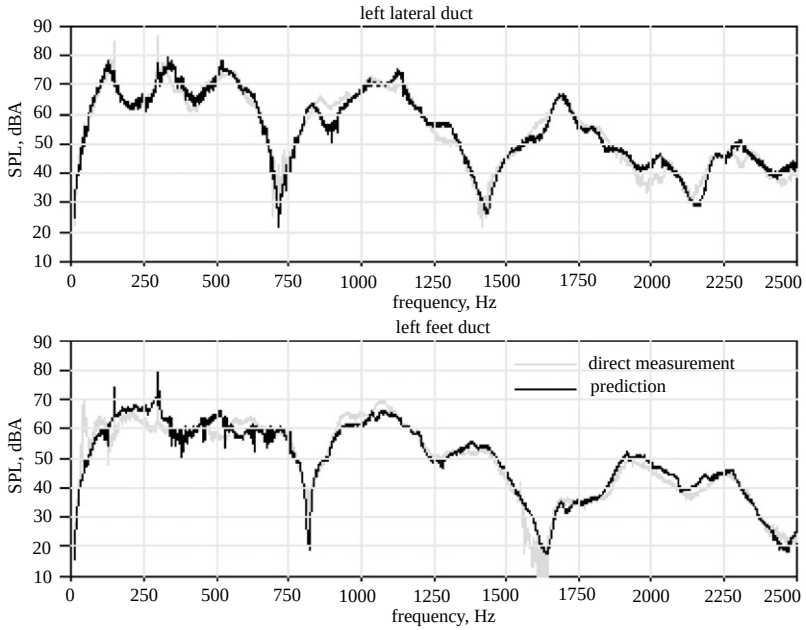

Fig. 6. Predicted and directly measured spectra at the end of the lateral and the floor-level ventilation ducts.

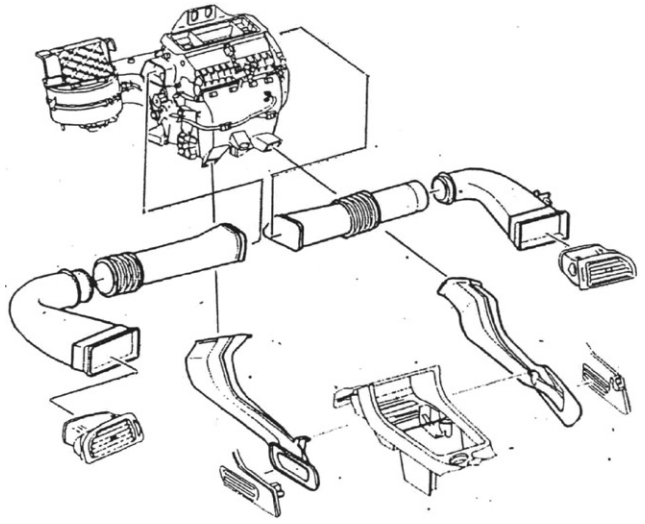

Fig. 7. The air-conditioning box and the four ventilation ducts.

condition is verified provided a few precautions are taken. This hypothesis is actually fulfilled for the lateral and the floor-level ducts, but it is not the case for the two defrosting ducts. However, the defrosting duct entrance sections are considerably smaller than those at the exit and also

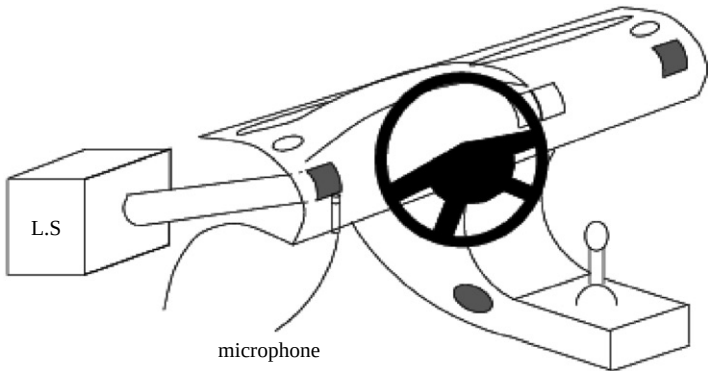

Fig. 8. Measurement of the transfer paths between an air outlet and the target points.

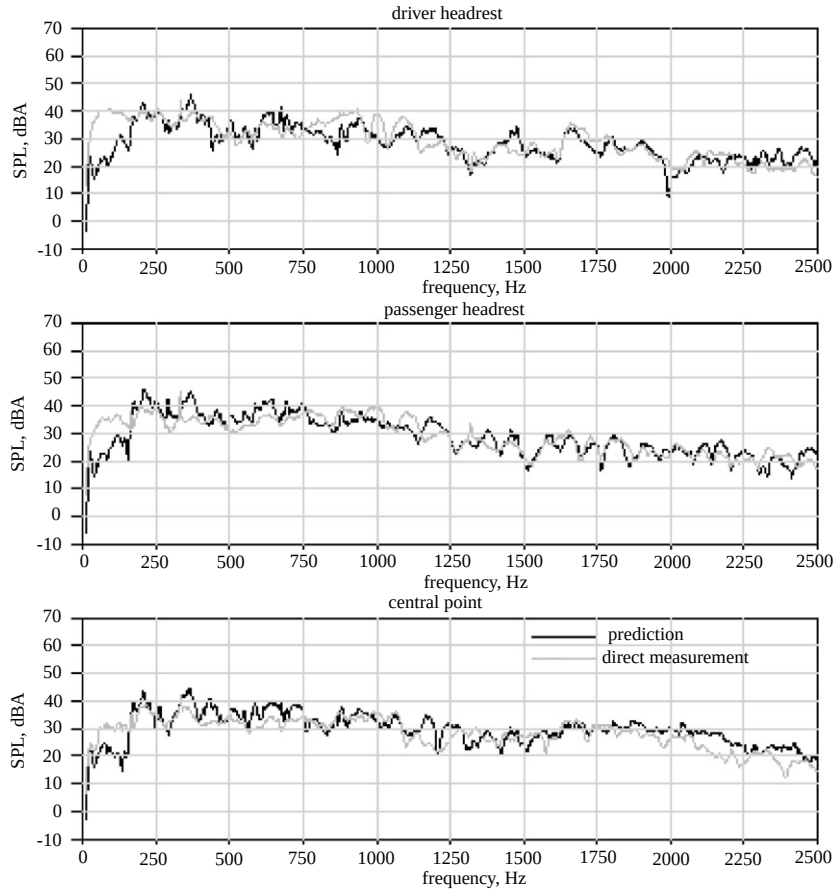

Fig. 9. Pressure levels predicted and measured directly at the target points.

smaller than the wavelength, which means that the plane-wave contribution is much greater than that of the other modal amplitudes at the duct entrances (which are also the air-conditioning box exits). This is why the multi-port source model is also appropriate for the defrosting exits of the

air-conditioning box. In this section, defrosting will be studied independently of aeration, and as there are two defrosting ducts on the test vehicle, the present source is a two-port one.

In order to extend the predictive methodology to the case of complex ducts with modal propagation several adjustments are necessary. Firstly, multi-modal impedance matrices have to be transferred from the duct exits back to the entrances and the plane-wave component has to be extracted to obtain the load impedances. Secondly, the pressure at the air-conditioning box exits calculated thanks to Eq. (12) must be propagated through the defrosting ducts to the nozzles, where the acoustic pressure is established on several modes. Various methods can be used to do these operations. The finite element method, which is universal, fits any geometry. Although very adaptable, it requires a variational description of the acoustic problem. The only acoustic variable is the pressure but the impedance transfer can be done using elementary properties of linear algebra. However, to keep close to what was done in the case of 1-D, it was decided to start with the finite stairs method, whereby the differential equations are directly solved by modal decomposition and the acoustic variables become vectors of pressure and velocity modal amplitudes. By analogy, the matrix which links the pressure modal amplitudes vector to that of the velocity is called the modal impedance matrix. The duct geometry is approximated by a succession of elementary elements (for instance, simple section discontinuities and straight guides) along the privileged propagation direction, and the impedance back-transfer is thus achieved step-by-step [13].

4.1. Integration of the finite stairs method into the predictive methodology

Only the broad outlines of the classic finite stairs method are given here before tackling the problem of characterizing the main cavity Ω_4. Indeed, considering the defrosting duct exit sections which are considerably larger than those of the 1-D ducts, both the radiation impedance calculation and the transfer path measurements are more complex.

4.1.1. The finite stairs method

The relation between the modal amplitude vectors at the entrance and at the exit of a guide can only be calculated for simple geometries such as rectilinear elements or simple area discontinuities, as far as analytical methods are envisaged. This explains why, with the finite stairs method, the duct geometry is approximated by a succession of stair steps, the length of which must be small enough in relation to the wavelength for the sound propagation inside such a discontinuous duct to resemble closely that observed in the real duct.

The modal decomposition of acoustic pressure and velocity in a section of a rectilinear element gives

$$\begin{aligned} p(x,y,z) &= \mathrm{i}\rho\omega \sum_n \left(a_n \mathrm{e}^{-\mathrm{i}k_n x} + b_n \mathrm{e}^{ik_n x}\right)\phi_n(y,z) = \mathrm{i}\rho\omega \langle \phi_n \rangle \{p_n\} = \mathrm{i}\rho\omega \quad \boldsymbol{\phi}^{\mathrm{t}} \cdot \boldsymbol{\pi}, \\ v(x,y,z) &= \mathrm{i} \sum_n k_n \left(a_n \mathrm{e}^{-\mathrm{i}k_n x} - b_n \mathrm{e}^{\mathrm{i}k_n x}\right)\phi_n(y,z) = \langle \phi_n \rangle \{v_n\} = \boldsymbol{\phi}^{\mathrm{t}} \cdot \mathbf{v}, \end{aligned} \tag{16}$$

where $\phi_n(y,z)$ is the nth transversal eigenfunction of the guide. Modal amplitude vectors $\boldsymbol{\pi}$ and $\mathbf{v}$ are the state variables. Equation $\boldsymbol{\pi} = \mathbf{Z} \cdot \mathbf{v}$ defines the modal impedance matrix $\mathbf{Z}$. The vectors and the matrix are theoretically of infinite size but in practice, they are truncated to a certain number N of modes.

The modal impedance matrix $\mathbf{Z}_{out}$ at the exit of the rectilinear element of length L can be transferred back to the entrance with the following equation [14]:

$$\mathbf{Z}_{in} = \frac{1}{\mathbf{k}\,\tan(\mathbf{k}L)} - \frac{1}{\mathbf{k}\,\sin(\mathbf{k}L)}\left(\mathbf{Z}_{out} + \frac{1}{\mathbf{k}\,\tan(\mathbf{k}L)}\right)^{-1}\frac{1}{\mathbf{k}\,\sin(\mathbf{k}L)},$$

where $\mathbf{k}$ is the diagonal matrix of wave numbers k_n. Then the velocity modal vector can be propagated from the duct entrance to the exit:

$$\mathbf{v}_{out} = k\,\sin(\mathbf{k}L)\quad\left(\mathbf{Z}_{in} + \frac{1}{\mathbf{k}\,\tan(\mathbf{k}L)}\right)\ \mathbf{v}_{in}.$$

These expressions are not the most straightforward available, but they allow the problem of numerical instability to be overcome.

Considering the whole discontinuous guide, elementary straight duct elements are connected to each other by applying the pressure and velocity continuity equations so as to be able to transfer back the modal impedance and to propagate the modal velocity vector.

4.1.2. Radiation modal impedance matrix at the defrosting nozzles

The radiation modal impedance matrix at a duct exit takes into account the main cavity response, and it was decided to calculate rather than measure it. Thus, in the case of a single defrosting nozzle of section Γ_b, term (n,q) of radiation modal impedance matrix $\mathbf{Z}_b$ is [13]

$$Z_{nq} = \frac{\mathrm{i}\omega\rho}{\Lambda_n}\int_{\Gamma_b}\mathrm{d}y'\,\mathrm{d}z'\phi_q(y',z')\int_{\Gamma_b}\mathrm{d}y\mathrm{d}z g_4(y,z,y',z')\phi_n(y,z), \tag{17}$$

where g_4 is the cavity Ω_4 Green function. The latter can only be calculated analytically in certain specific cases, for instance if Ω_4 can be assimilated to a half-space limited by an infinite rigid plane.

With the defrosting ducts, the exit sections of which are Γ_b and Γ_d, the radiation modal impedance matrix is defined by

$$\begin{Bmatrix}\boldsymbol{\pi}_b\\ \boldsymbol{\pi}_d\end{Bmatrix} = [Z_4]\begin{Bmatrix}\mathbf{v}_b\\ \mathbf{v}_d\end{Bmatrix},$$

where π_j and v_j are, respectively, the modal pressure and velocity vectors on section Γ_j. In the present work, the mutual influences of one duct exit section on the other have been ignored, so the radial modal impedance matrix is

$$[Z_4] = \begin{bmatrix}\mathbf{Z}_b & 0\\ 0 & \mathbf{Z}_d\end{bmatrix}.$$

4.1.3. Transfer paths measurement between the defrosting nozzles and the target points in Ω_4

To obtain a complete characterization of the main cavity Ω_4, the transfer paths between the defrosting nozzles and the target points in the passenger cavity must be determined. Previously, when the only propagative mode in the ducts was the plane wave, these transfer paths were

characterized by transfer functions. Now, considering the dimensions of the duct exit sections, another approach will achieve the goal.

The acoustic operator of cavity Ω_4 with non-zero velocity fields on sections Γ_b and Γ_d is

$$\begin{aligned} &Hp(\mathbf{x}) = 0 && \text{in } \Omega_4,\\ &p_{,n} = -\mathrm{i}\rho ckv_b && \text{on } \Gamma_b,\\ &p_{,n} = -\mathrm{i}\rho ckv_d && \text{on } \Gamma_d,\\ &p_{,n} + \mathrm{i}k\beta_4 p = 0 && \text{on } \partial\Omega_4 \setminus (\Gamma_b \cup \Gamma_d). \end{aligned} \tag{18}$$

The associated boundary equation for a point $\mathbf{x}_4$ of the passenger compartment is

$$p(\mathbf{x}) = -\int_{\Gamma_b \cup \Gamma_d} g(\mathbf{x}, \mathbf{x}') p_{,n}(\mathbf{x}')\, \mathrm{d}\mathbf{x}' = -\mathrm{i}\rho ck \int_{\Gamma_b \cup \Gamma_d} g(\mathbf{x}, \mathbf{x}')\, v(\mathbf{x}')\, \mathrm{d}\mathbf{x}'. \tag{19}$$

By splitting sections Γ_b and Γ_d into a number N_{esc} of elementary sections Γ_j, and by approximating the acoustic velocity distribution on Γ_b and Γ_d by a curve V_{esc} which is constant on the elementary sections Γ_j, the previous equation becomes

$$p(\mathbf{x}) = -\sum_{j=1}^{N_{esc}} v_{\mathrm{esc}}^j R_j(\mathbf{x}) \quad \text{where } R_j(\mathbf{x}) = \mathrm{i}\rho ck \int_{\Gamma_j} g(\mathbf{x}, \mathbf{x}')\, \mathrm{d}\mathbf{x}'$$

Note that only the value of the acoustic velocities v_{esc}^j counts here, and not the modal amplitudes of the velocity. This remark could give an advantage to the finite element method over the finite stairs method.

The transfer path parameters are thus the transfer impedances $R_j(\mathbf{x}_4)$ which are measured using an external loudspeaker connected successively to the rear of each elementary section, while the rest of the ducts exit sections are rigidly closed. The transfer impedance is then the ratio of the pressure measured on a target point to the velocity on the elementary section Γ_j. The latter is again the ratio of the measured pressure on Γ_j to the impedance at the same point. The impedance is measured with a two microphone antennae to apply the transfer function technique [5]. The experimental set-up is shown in Fig. 10.

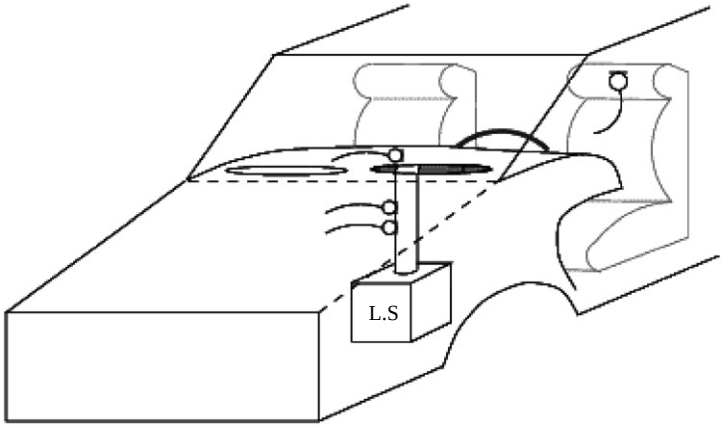

Fig. 10. Experimental setting for the transfer impedances $R_j(\mathbf{x}_4)$ measurement.

Numerical simulations have been carried out in order to evaluate the influence of two major approximations of the method. Firstly, the fact that the velocity distributions on the defrosting nozzles are approximated by curves which are constant on a number N_{esc} of elementary sections may cause errors. The simulations indicate that if N_{esc} is equal to or even greater than the number of modes in the finite stairs model, the impact of the velocity distribution decomposition on the prediction is small. Secondly, an approximation is done to calculate the radiation modal impedance matrix. According to the numerical simulation results, the hypothesis of radiation in a half-space instead of a cavity leads to error peaks. The more absorbent the cavity, the lesser the peaks.

4.2. Experimental results

An experiment on a vehicle was carried out to validate the methodology for predicting sound levels at target points in the passenger compartment, caused by the propagation of ventilator noise through the two defrosting ducts. The source strength and impedance matrices $\mathbf{S}_s$ and $\mathbf{Z}_s$ were extracted from the measurements on the global six-port source made up of the conditioning box at the lateral, floor-level and defrosting exits. The target points in the passenger compartment are the same as in Section 3.3.2.

The finite stairs model of the two defrosting ducts takes into account all the propagative modes and five evanescent modes. The viscothermal losses were taken into account. The duct geometry is shaped with 30 stair steps on their whole length of 11 cm. The calculations were made in the frequency range from 100 to 2000 Hz with steps of 10 Hz.

To measure the transfer impedance, each defroster nozzle section was split into 11 elementary sections of 3.5 cm length. Moreover, the transfer impedance was also measured between the two defroster nozzles and the target points.

Direct measurements of the sound pressure spectra at the three target points due to defrosting have also been done and are seen as reference curves for the evaluation of the predictive method accuracy. Results are given in Fig. 11.

Although the main trends are respected, the results are less satisfactory than those obtained with the 1-D ducts. Three main factors may be the cause. Firstly, the defrosting noise was measured in presence of the air outlets whereas the prediction does not take into account the noise generated by the impact of flow noise on the flanges. The predicted noise is lower than that measured at high frequencies, which is typically the frequency range of a noise generated by pressure turbulent fluctuations on an obstacle. Secondly, the defrosting duct is difficult to model due to the fact that it splits into two at the exit. Lastly, a drastic simplification of the cavity response was made to calculate the diagonal radiation modal impedance matrix and this may be responsible for the error peaks.

5. Conclusion

Considering the acoustical and geometrical complexity of the air-conditioning box and passenger compartment, a complete model of the automotive air-conditioning system from the fan to the passengers' ears is still inconceivable. For the time being, a predictive approach can only

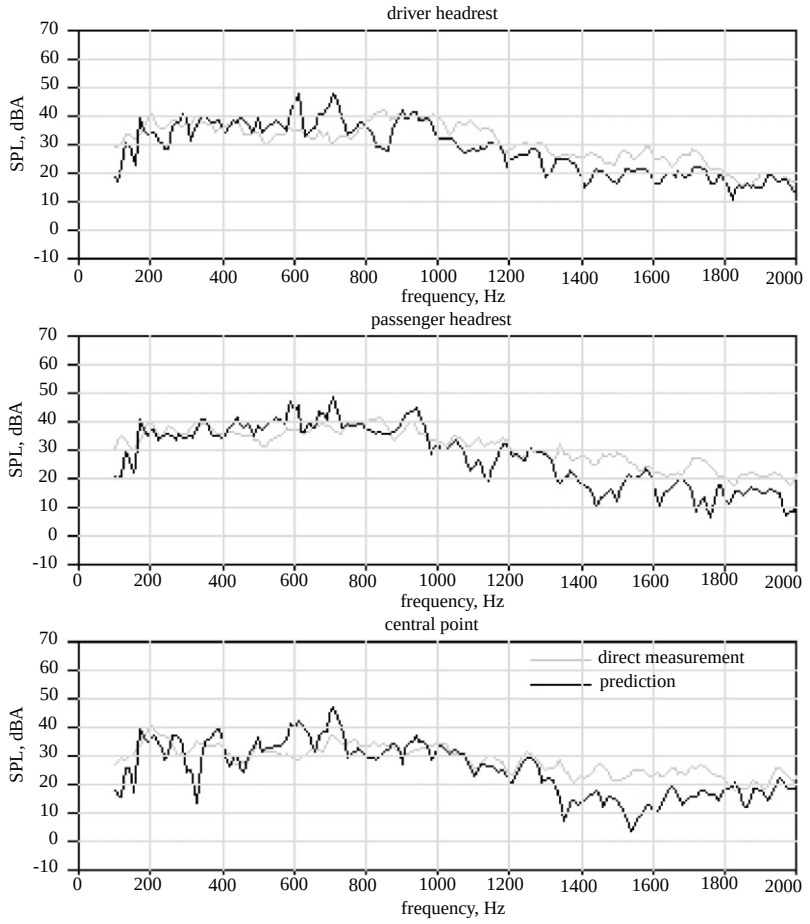

Fig. 11. Predicted and directly measured pressure spectra at the three target points of the passenger compartment.

be undertaken insofar as the acoustical behaviour of the ducts is well-mastered and can be calculated, while measurements describe the acoustic behaviour of the two cavities isolated from the rest of the system. Calculations then couple the domains.

The conditioning box, with its exits towards aeration and defrosting ducts constitutes a six-port source. Here aeration and defrosting have been dealt with separately. The prediction relies on the identification of source parameters and on the description of the passenger compartment behaviour by a diagonal load impedance matrix considering distant outlets and defrosting nozzles, and acoustic absorption, perhaps a fragile hypothesis for low frequencies.

Through a progressive procedure the experimental validation shows the influence of the increasing complexity of the system on predictive accuracy. Very good experimental results were first obtained when a conditioning box with only three exits connected to straight ducts radiated in an anechoic chamber. The acoustic behaviour of each port independent of the loads

applied to the others emphasizes the diagonality of both source impedance and load impedance matrices, a property lost in later results when the conditioning box exits are located close to each other.

Then, dealing with aeration noise, i.e., with four exits of the conditioning box radiating into the passenger compartment via plane waveguides, the results, although convincing, have lost the quality observed previously, probably because the air jet noise was absent from the preliminary measurements, the radiation impedance matrix was not diagonal for low frequencies and errors may have occurred in modelling the car ducts and compartment.

Lastly, concerning predictions of noise through defrosting ducts, the trends remain but the results are less satisfactory than for the previous configurations, for the same reasons as before and with greater consequences. Therefore, further investigation is needed: measurements of flow noise generated at the outlet flanges, validation of the defrosting ducts finite stairs model either experimentally or by comparison with a finite element model and improvements in the radiation modal impedance matrix to prove whether it could bring about significant gains in predictive accuracy.

Despite these shortcomings, the validity of the strategy has been shown experimentally and fully justifies optimism about improving predictive accuracy in these complex technological situations. The parameter setting of this model according to the duct shapes and materials now opens perspectives for the design of acoustically optimized ventilation ducts according to attenuation criteria defined on target ranges of frequencies.

Finally, with what degree of realism is it possible to extend the prediction made for un-built cars based in part on measured data from existing vehicles? This question, which was asked by a referee of this paper, concerns two possible definitions of an ''un-built'' car. In the first case, it may be a car belonging to the same series as the existing vehicle(s). Here it would be possible to guarantee a sound level in the passenger' compartment from the prediction in the existing vehicle and the known acoustic characteristic dispersion of the series. This type of procedure has already given realistic results in active noise control to define a guaranteed minimal attenuation (Gronier–Martin). On the other hand, un-built car may also be even slightly different from the existing vehicle. What would then be the variations in the measured acoustic behaviour of the cavities, in the absence of a sufficiently precise numerical model, in particular for the conditioning box? At present no answer can be given. However, a possible direction to investigate could be further research based on the comparisons between different acoustic fields resulting from the use of different methods to deal with the same acoustic problem (Courtois–Martin): more similarity has been observed in the variations of a field due to a modification in the configuration than in the field itself in the initial configuration. This could perhaps lead the way to changing the measured characteristics with the help of variations calculated on a simple numerical model of the existing vehicle modified to simulate the future car. As far as we know, such research has not yet been carried out.

Acknowledgements

The authors wish to thank the Faurecia SARL for having authorized the publication of results obtained on their equipment.

References

[1] C.L. Morfey, Sound transmission and generation in ducts with flow, Journal of Sound and Vibration 14 (1971) 37–55.
[2] M.L. Kathuriyan, M.L. Munjal, Experimental evaluation of the aeroacoustic characteristics of a source of pulsating gas flow, Journal of Acoustical Society of America 65 (1979) 240–248.
[3] H. Boden, Error analysis for the two-load method, Journal of Sound and Vibration 126 (1988) 173–177.
[4] M.G. Prasad, M.J. Crocker, Acoustical source characterization studies on a multi-cylinder engine exhaust system, Journal of Sound and Vibration 90 (1983) 479–508.
[5] J.Y. Chung, D.A. Blaser, Transfer function method of measuring in-duct acoustic properties, Journal of Acoustical Society of America 68 (1980) 907–921.
[6] C.W.S. To, A.G. Doige, A transient testing technique for the determination of matrix parameters of acoustic systems, Journal of Sound and Vibration 62 (1979) 207–233.
[7] M.G. Prasad, M.J. Crocker, A scheme to predict the sound pressure radiated from an automotive exhaust system, Journal of Acoustical Society of America 70 (1981) 1345–1352.
[8] J. Lavrentjev, M. Abom, H. Boden, A measurement method for determining the source data of acoustic two-port sources, Journal of Sound and Vibration 183 (3) (1995) 517–531.
[9] M. Terao, H. Sekine, Fan acoustical characteristics required for reliable HVAC duct sound prediction, Proceedings of Fan Noise Symposium, CETIM, France, 1992, pp. 359–364.
[10] H.S. Alves, A.G. Doige, A three load method for noise source characterization in ducts, Noise-Conference '87, 1987, pp. 329–334.
[11] M.G. Prasad, A four load method for evaluation of acoustical source impedance in ducts, Journal of Sound and Vibration 114 (1987) 247–356.
[12] B.S. Shridhara, M.J. Crocker, Error analysis for the four-load method used to measure the source impedance in ducts, Journal of Acoustical Society of America 92 (5) (1992) 2924–2931.
[13] A.Roure, Propagation guidée, étude des discontinuités, Thèse de doctorat, Université d'Aix-Marseille II, 1976.
[14] A. Roure, Propagation du son dans des conduits à section continuement variable. Application à la détermination des fréquences propres de certains volumes complexe, Proceedings of Euromech '94, CNRS-LMA, France, 1977, pp. 1–10.